JOURNAL OF VIROLOGY, Mar. 2011, p. 2512–2523 Vol. 85, No. 6
0022-538X/11/$12.00 doi:10.1128/JVI.01160-10

Ebolavirus Proteins Suppress the Effects of Small Interfering RNA by Direct Interaction with the Mammalian RNA Interference Pathway▽

Giulia Fabozzi,[1]† Christopher S. Nabel,[1]† Michael A. Dolan,[2] and Nancy J. Sullivan[1]*

Biodefense Research Section, Vaccine Research Center,[1] and Bioinformatics and Computational Biosciences Branch, Office of Cyber Infrastructure and Computational Biology,[2] National Institute of Allergy and Infectious Disease, National Institutes of Health, Bethesda, Maryland 20892

Received 31 May 2010/Accepted 24 December 2010

Cellular RNA interference (RNAi) provides a natural response against viral infection, but some viruses have evolved mechanisms to antagonize this form of antiviral immunity. To determine whether Ebolavirus (EBOV) counters RNAi by encoding suppressors of RNA silencing (SRSs), we screened all EBOV proteins using an RNAi assay initiated by exogenously delivered small interfering RNAs (siRNAs) against either an EBOV or a reporter gene. In addition to viral protein 35 (VP35), we found that VP30 and VP40 independently act as SRSs. Here, we present the molecular mechanisms of VP30 and VP35. VP30 interacts with Dicer independently of siRNA and with one Dicer partner, TRBP, only in the presence of siRNA. VP35 directly interacts with Dicer partners TRBP and PACT in an siRNA-independent fashion and in the absence of effects on interferon (IFN). Taken together, our findings elucidate a new mechanism of RNAi suppression that extends beyond the role of SRSs in double-stranded RNA (dsRNA) binding and IFN antagonism. The presence of three suppressors highlights the relevance of host RNAi-dependent antiviral immunity in EBOV infection and illustrates the importance of RNAi in shaping the evolution of RNA viruses.

RNA interference (RNAi) is a sequence-specific gene regulatory pathway widely conserved from plants to mammals (16, 47) that provides a natural cellular response to viral infection. Since mammals have evolved complex protein-based adaptive and innate immunity in response to infection, the existence of a nucleic acid-based innate immunity such as RNAi was initially debated. To date, several studies have provided experimental support to clarify the role of RNAi-based immunity in mammals. The identification of proteins working as suppressors of RNAi in animal virus (38) and of noncoding adenoviral RNAs able to inhibit components of the RNAi machinery (64) as well the presence of virus-derived small RNAs (3, 11, 48) and the observation that engineered RNAi can successfully restrict viral infection in mammalian cells (4, 17, 18, 28, 31) support a role for RNAi as an innate antiviral mechanism (3, 11, 38, 48).

The first mechanistic step of the RNAi pathway involves Dicer, an RNase III-type enzyme that processes double-stranded RNAs (dsRNAs) into small interfering RNAs (siRNAs) of 19 to 21 nucleotides (nt) in length, with 2-base 3′ overhangs (12, 16, 41, 47). The RNA-induced silencing complex (RISC) unwinds duplex siRNAs and selectively incorporates one strand of the pair, known as the guide strand. In the active RISC, the guide strand identifies the target RNA transcript (mRNA) with perfect sequence complementarity. The endonuclease Argonaute2 (Ago2) then cleaves and disrupts the targeted transcript (41). The active RISC includes Dicer, Ago2, TRBP, and PACT. TRBP and PACT are two dsRNA-binding proteins (dsRBPs) that function as partners for Dicer (29), forming a complex with Dicer and Ago2 to achieve siRNA-mediated cleavage of mRNA and facilitate microRNA (miRNA) biogenesis (6, 19, 20, 33). TRBP and PACT also bind the dsRNA-dependent protein kinase R (PKR), which phosphorylates the α translation factor eIF-2, thereby inhibiting protein synthesis and activating the interferon (IFN) response to dsRNA (46). TRBP inhibits PKR, while PACT positively regulates PKR. Therefore, RNAi- and PKR-mediated pathways may overlap each other by sharing either the common trigger (dsRNA) or effectors of dsRNA surveillance.

In response to host RNAi-dependent immunity, viruses have evolved several countermeasures (reviewed in references 20 and 68). Both plant and animal viruses encode protein suppressors of RNA silencing (SRSs) (65). Examples of mammalian SRSs are the human immunodeficiency virus type 1 Tat factor (3, 40) and the dsRBP/IFN antagonists influenza A virus NS1 and vaccinia virus E3L (40). While SRSs are relatively well characterized in plant and insect models, the function of mammalian RNAi inhibitors is the subject of debate (9, 61) and the underlying molecular mechanism of dsRBP/IFN RNAi inhibitors remains poorly understood (21, 40). Haasnoot et al. (21) postulated that Ebolavirus (EBOV) VP35 functions as an SRS based on two known properties, dsRNA binding and IFN antagonism, since dsRNA binding-defective mutants abolish short hairpin RNA (shRNA) RNAi suppression (21). However, the molecular mechanism by which EBOV VP35 interacts with the RNAi pathway has not yet been elucidated.

EBOV (family *Filoviridae*, order *Mononegavirales*) is a nonsegmented negative-strand (NNS) RNA virus. The RNA negative-strand genome is associated with the nucleocapsid proteins NP, VP30, VP35, and L, an RNA-dependent RNA polymerase (RdRp), to form the ribonucleoprotein (RNP) complex, which participates in viral replication and transcrip-

* Corresponding author. Mailing address: National Institutes of Health, Vaccine Research Center, 40 Convent Drive, Bldg. 40/2509, Bethesda, MD 20892. Phone: (301) 435-7853. Fax: (301) 480-2771. E-mail: njsull@mail.nih.gov.

† These authors contributed equally to this work.

▽ Published ahead of print on 12 January 2011.

tion (14). As is the case with other NNS viruses, EBOV replication and transcription take place in the cytoplasm. Based on the vesicular stomatitis virus as a model for NNS viruses (63), following viral entry into the cytosol, the RNP complex-associated genome is uncoated and exposed to RdRp to be immediately transcribed into a short, uncapped, positive-stranded RNA leader and seven-capped and polyadenylated mRNAs, which encode the viral proteins necessary for replication (63). To maximize viral replication and transmission in the infected host, EBOV has evolved mechanisms that effectively subvert the host immune system. EBOV evades the cytosolic pathways that discriminate self-RNA (capped) from non-self-RNA (uncapped) by having capped and polyadenylated mRNAs. Once in the cytosol, however, EBOV can be recognized by host pattern recognition receptors (PRRs), such as the retinoic acid-inducible gene I (RIG-I), which is known to sense 5′ triphosphate (5′ppp) single-stranded RNA (ssRNA) (22, 26) as well as 5′ppp-bearing short dsRNA (52).

EBOV may also subvert dsRNA recognition pathways by limiting dsRNA formation through coating the RNAs with nucleocapsid proteins, which prevent the positive- and negative-stranded RNAs from annealing (1). However, a panhandle-like dsRNA structure is predicted to form due to a high degree of complementarity of the 3′ and 5′ ends of the EBOV genome (62). In the case of rabies virus, short dsRNA panhandles bearing 5′ppp activate RIG-I (52) and form a complex with the receptor (53).

In this study, we designed siRNAs that successfully silenced transiently expressed EBOV genes. However, these siRNAs did not show complete silencing of EBOV genes during active viral replication. This led us to hypothesize that the virus actively resists cellular RNAi during replication. To identify how EBOV inhibits RNAi, we used a reporter-based RNAi assay to screen the effects of all viral products and found three EBOV proteins, VP30, VP35, and VP40, that function independently as SRSs. Of these proteins, two are components of the viral RNP complex. Additionally, we found that VP30 and VP35 associate with the RNAi machinery, whereas VP40 does not, suggesting an independent mechanism for this protein. Here, we present the molecular mechanisms of VP30 and VP35. Our findings elucidate a novel mechanism used by EBOV to actively evade host responses that block EBOV pathogenicity.

MATERIALS AND METHODS

Virus. The EBOV Zaire species (Mayinga isolate, GenBank accession no. AY354458) was used to infect Vero cells at a multiplicity of infection (MOI) of 0.2. Infection experiments were performed under biosafety level 4 (BSL4) containment fully accredited by the American Biological Safety Association.

Plasmids. Plasmids encoding green fluorescent protein (pGFP) and those encoding the EBOV proteins NP, GP, VP30, VP35, and VP40 are derived from plasmid VR1012 (24, 57); pVP30, pVP35, and pVP40 were also constructed with a C-terminal FLAG epitope (DYKDDDDK) by site-directed PCR mutagenesis using a QuikChangeXL site-directed mutagenesis kit (Stratagene, La Jolla, CA). pVP35 and pVP30 were engineered with a C-terminal six-histidine (6×His) tag by site-directed mutagenesis. All mutants of VP35 and VP30 were generated by using the correspondent His-tagged wild-type plasmid. Primers were designed to introduce the site-directed mutations K309A and R132A for VP35 and R40A for VP30 according to the literature (21, 27). The constructs pVP30 C1 (configuration 1), carrying the mutations D158A, T161A, E163A, D164A, and S165A, pVP30 C2 (configuration 2), having D202A and E205A, and pVP30 C3 (configuration 3), with H215A and S216A, have been generated by site-directed mutagenesis. The mutations were confirmed by DNA sequencing, and protein expression was confirmed by Western blot analysis. Deletion mutant VP30Δ1-40 (with the region encompassing residues 1 to 40 deleted) was generated by standard PCR- and cloning-based methods. pCMVLacZ and FLAG-pCMV luciferase, encoding β-galactosidase (β-Gal) and luciferase enzymes, respectively, were from Stratagene. The plasmid encoding FLAG-Ago2 (plasmid 10822) was from Addgene (45), and those encoding the FLAG-Dicer, FLAG-PACT, and FLAG-TRBP proteins were provided by Narry K. Kim, Institute of Molecular Biology and Genetics, Seoul National University, Seoul, South Korea.

siRNAs. siRNAs were chemically synthesized by Dharmacon (ThermoFisher, Lafayette, CO). The sequences of the siRNAs designed in this study, reported as sense strand and with respect to the viral mRNA, are as follows: for the siRNA targeting NP (siNP), 5′-GGCAAAUUCAAGUACAUGCdTdT-3′ (NP mRNA, 520 to 539 nt); for siNP5, 5′-GCAUGGAGAGUAUGCUCCUdTdT-3′ (NP mRNA, 866 to 885 nt); for siGP4, 5′-ACCUGACGGGAGUGAGUGUdTdT-3′ (GP mRNA, 344 to 363 nt); for siGP5, 5′-AGAGGGUGCUUUCUUCCUGd TdT-3′ (GP mRNA, 464 to 483 nt); and for siGFP, 5′-GGCUACGUCCAGG AGCGCACCdTdT-3′ (GFP mRNA, 274 to 294 nt). The ON-TARGET*plus* nontargeting siRNA #1 (D-001810-01) and the siGLO Red transfection indicator (D-001630-02) were from Dharmacon.

Cell culture and transfections. Human embryonic kidney HEK293 and African green monkey kidney Vero E6 cells were obtained from the American Type Culture Collection (ATCC, Manassas, VA) and cultured as per ATCC instructions without antibiotics. Cells were plated at a density of 0.5×10^6 cells/well in a 6-well plate.

Cotransfection of plasmid and siRNAs was carried out with Lipofectamine 2000 (11668-019; Invitrogen) as described by the manufacturer, and cells were incubated for 72 h posttransfection. siRNA transfection into Vero cells was carried out using Oligofectamine (12252-011; Invitrogen). siRNA duplex (300 pmol/well) was transfected, and after 4 h, cells were infected with EBOV Zaire at an MOI of 0.2 for 1 h. siRNA-EBOV-infected Vero cells were washed and incubated for 48 h posttransfection. Viral replication was tested by plaque assay. Transfections were performed in triplicate.

Reporter-based RNAi assay. The RNAi assay for SRS screening was performed in HEK293 cells by cotransfecting 0.025 μg pGFP alone, 0.025 μg pGFP together with 25 pmol of the nontargeting siRNA, 0.025 μg pGFP with 25 pmol of siGFP alone, or 0.025 μg pGFP together with 25 pmol of siGFP and 2 μg of each plasmid encoding the viral proteins. pCMVLacZ (0.05 μg) and siGLO Red (60 pmol) were added to the cotransfection mixture and used as plasmid DNA (pDNA) and siRNA transfection delivery controls, respectively. The GFP-based RNAi assay was modified to test a target other than GFP and used 0.010 μg of pGP and 5 pmol of siGP4. For fluorescence measurements, GFP or Cy3 fluorescence was measured using a SpectraMaxM2^e reader (Molecular Devices Inc., Sunnyvale, CA).

Western blotting. Transfected cells were harvested and resuspended in a Nonidet P-40-containing lysis buffer supplemented with protease inhibitor cocktail (11836153001; Roche Diagnostics, Mannheim, Germany). The total protein content was measured with Quick Start Bradford protein assay reagent (Bio-Rad, Hercules, CA), and samples were subjected to SDS-PAGE analysis followed by Western blotting.

Primary antibodies were monoclonal mouse anti-GFP from Covance (Princeton, NJ), monoclonal mouse anti-β-actin from Santa Cruz Biotechnology (Santa Cruz, CA), rabbit anti-β-galactosidase from Invitrogen, monoclonal mouse anti-FLAG M2 from Sigma (F3165; St. Louis, MO), monoclonal mouse anti-His from Qiagen (34660; Valencia, CA), monoclonal mouse anti-NP-9B8 from B. Haynes (Department of Immunology, Duke University, Durham, NC), and anti-GP-12B5 from M. K. Hart (Virology Division, U.S. Army Medical Research Institute of Infectious Diseases, Fort Detrick, Frederick, MD). Secondary antibodies were peroxidase-conjugated anti-mouse (sc-2053; Santa Cruz) and anti-rabbit (sc-2054; Santa Cruz). Bound antibodies were visualized by an enhanced chemiluminescence system (ECL Plus) according to the manufacturer's instructions (GE Healthcare, Amersham Biosciences, Pittsburgh, PA).

Type I interferon (IFN-α/β) ELISA. Samples from siRNA-transfected HEK293 cells were collected at 8, 24, and 48 h and used to measure human IFN-α/β by enzyme-linked immunosorbent assay (ELISA) according to the manufacturer's instructions (PBL Interferon Source, Piscataway, NJ). Poly(I · C) (P9582; Sigma) and poly(dA-dT) (Invivogen, San Diego, CA) were used as positive controls.

Gel band visualization and quantification. Immunoblot bands were acquired using an Epson Perfection 4870 Photo instrument (Epson, Long Beach, CA), and selected bands were quantified based on their relative intensities using ImageJ densitometry software (version 1.6; National Institutes of Health, Bethesda, MD).

Statistical analysis of Western blotting data. Densitometry values of the samples were evaluated for statistical significance. One-way analysis of variance (ANOVA) with Student-Newman-Keuls *t* test was performed with GraphPad

Prism software (version 5.02; GraphPad Software Inc., San Diego, CA). A P value of <0.05 was considered statistically significant.

Immunoprecipitation. To detect the interactions between EBOV SRSs and RNAi components, immunoprecipitations were carried out by incubating 3,500 μg of total cell lysates with 4 μg of antibodies to Dicer (polyclonal rabbit H-212 [sc-30226; Santa Cruz]), PACT (monoclonal mouse 2830c1a [sc-81569; Santa Cruz]), and TRBP (polyclonal rabbit [Ab42018; Abcam, Cambridge, MA]). Antibodies directed to the FLAG or the His tag were used in the coimmunoprecipitation experiments. Antibody-containing sample was mixed with 65 μl of Dynabeads G protein (100.04D; Invitrogen), and immunoprecipitations were carried out in accordance with the manufacturer's recommendations. Samples were subjected to SDS-PAGE followed by Western blotting with the anti-FLAG antibody and the specific antibody for detection of endogenous gene expression. For detection of TRBP, a mouse monoclonal TRBP antibody was used (S-11 [sc-100909; Santa Cruz]).

Protein-protein docking. The crystal structures of the C-terminal domain dimer of EBOV VP30 (Protein Data Bank identification no. [PDB ID] 2I8B) and the RNase IIIb domain dimer of human Dicer (PDB ID 2EB1) were obtained from the Protein Data Bank (30). Both structures were submitted to the Patchdock and GRAMMX protein-protein docking servers without including Mg ions for rigid, blind docking (54, 59). From each program, the top 10 docking solutions were returned based on lowest energy. All solutions were clustered based on a 5-Å root mean square (RMS) deviation between C_α atoms. Representative structures from all clusters were obtained.

Bioinformatic analysis of αββββα topology for EBOV SRSs. The EBOV VP30, VP35, and VP40 sequences (GenBank accession no. AY345548) were used to predict the presence of a dsRNA binding domain (dsRBD) with the classic αββββα topology. The RNase III dsRBD from *Thermotoga maritima* (Uniprot accession no. Q9X0I6), containing the αββββα architecture, was used as a positive control.

Secondary-structure predictions of VP30, VP35, and VP40 were performed with the meta-server at NPS (Network Protein Sequence Analysis) (8), JPred3 (7), PSIPRED PORTER (49), and PROFsec (51).

RESULTS

RNA silencing of EBOV genes expressed as cDNA-driven or viral transcripts. To evaluate RNAi targeting of EBOV genes, we designed several siRNAs complementary to different viral genes. Before testing our siRNAs in the context of active infection, we first verified the potency of candidate siRNAs against EBOV cDNA sequences expressed in cultured cells. We coexpressed the nucleoprotein (NP) or the glycoprotein (GP) in human kidney cells, HEK293, alone or together with a nontargeting control siRNA or with siRNAs specifically targeting each viral mRNA. A nontargeting siRNA did not alter expression of either GP or NP EBOV genes (Fig. 1A). In contrast, siNP2 and siNP5, as well as siGP4 and siGP5, completely silenced NP and GP gene expression, respectively, compared to the nontargeting siRNA control.

To rule out that the observed silencing involved a factor unique to this particular cell line, we repeated the experiment in monkey Vero cells. As observed in HEK293 cells, siNP and siGP treatment completely silenced transient EBOV gene expression in monkey Vero cells (Fig. 1B). Together, these results demonstrate that exogenously delivered siRNAs successfully knock down *in vitro* EBOV gene expression in two independent cell lines with equivalent efficacies.

To test siRNA-mediated RNA silencing during viral replication, we transiently transfected Vero cells with GP- or NP-specific siRNAs under the same conditions used to assess siRNA effects on cDNA products and, after 4 h, infected the cells with EBOV at a multiplicity of infection (MOI) of 0.2. Since assays for the measurement of viral protein are not routinely performed in biosafety level 4 (BSL4) containment, where this experiment was conducted, we instead evaluated viral load by plaque assay to assess the efficiency of siRNA silencing. Unlike the results showing efficient silencing of transiently expressed cDNA, transfection of siNPs and siGPs reduced virus replication in siRNA-treated cells only modestly (Fig. 1C). EBOV infection of Vero cells was reduced by a maximum of about 60% after siRNA treatment, regardless of the targeted gene. To our surprise, the suppression of viral replication in EBOV-infected cells by siRNAs was less effective than we had expected given our observations of their effect on individual EBOV genes expressed by transfection. Several mechanisms could explain the lack of inhibition of EBOV by RNAi seen in Fig. 1C. Among these, we considered potential limitations offered by the mode of siRNA delivery. However, we reasoned that EBOV biology could provide alternative explanations and speculated that EBOV has evolved one or more mechanisms to circumvent the cellular RNAi response. EBOV could escape RNAi through mutations of regions targeted by siRNAs, or viral RNA regions could be highly structured and therefore inaccessible to the RNAi machinery. The fact that EBOV replicates rapidly could also affect timely and efficient RNAi. Lastly, since many pathogen-encoded proteins interact directly with host cell antiviral responses, we chose to pursue the hypothesis that EBOV proteins functionally intersect the RNAi pathway.

EBOV proteins suppress siRNA-mediated RNAi. Upon entry into the cell, EBOV delivers its RNA genome wrapped within an RNP complex (NP, VP30, VP35, and L). Therefore, it is possible that the virus uses any member of the RNP complex to suppress RNAi during early stages of infection. To test this hypothesis, we employed a GFP reporter-based RNAi assay in HEK293 cells in which we cotransfected a plasmid carrying one of the viral genes together with 0.025 μg of the reporter plasmid pGFP and 25 pmol of the siRNA targeting GFP (siGFP) and then measured the level of GFP after 72 h. Any viral protein that reverted silencing of the reporter gene was considered a suppressor of RNAi. Because the reversion of silencing was achieved by simultaneous transfection of plasmids and siGFP, we verified that the plasmid DNA and siRNAs were efficiently delivered by using a plasmid expressing β-galactosidase (β-Gal) as a transfection control to normalize GFP expression (data not shown) and a second, nontargeting Cy3-labeled RISC-free siRNA to assess the efficiency and stability of siRNA delivery by assessment of Cy3 fluorescence (data not shown). Expression of different EBOV gene products in the GFP reporter-based RNAi assay revealed three SRSs (Fig. 2A). In the presence of siGFP, GFP expression was reduced by nearly 80% compared to GFP expression levels in the presence of a nontargeting siRNA. Two components of the viral RNP complex, VP30 and VP35, decreased siGFP-mediated silencing 2.5-fold when coexpressed individually with pGFP and siGFP. In contrast to VP30 and VP35, another member of the RNP complex, NP, did not reverse silencing. During the screening, we found serendipitously that VP40 also functioned as an SRS. Coexpression of VP40 together with the reporter plasmid and siGFP reverted silencing to the same degree as VP30 or VP35 (Fig. 2B). GP and VP24 (not members of the RNP complex) did not reverse GFP silencing (data not shown).

Since synthetic siRNAs have the potential under certain conditions to induce IFNs (50) and, moreover, since one of the

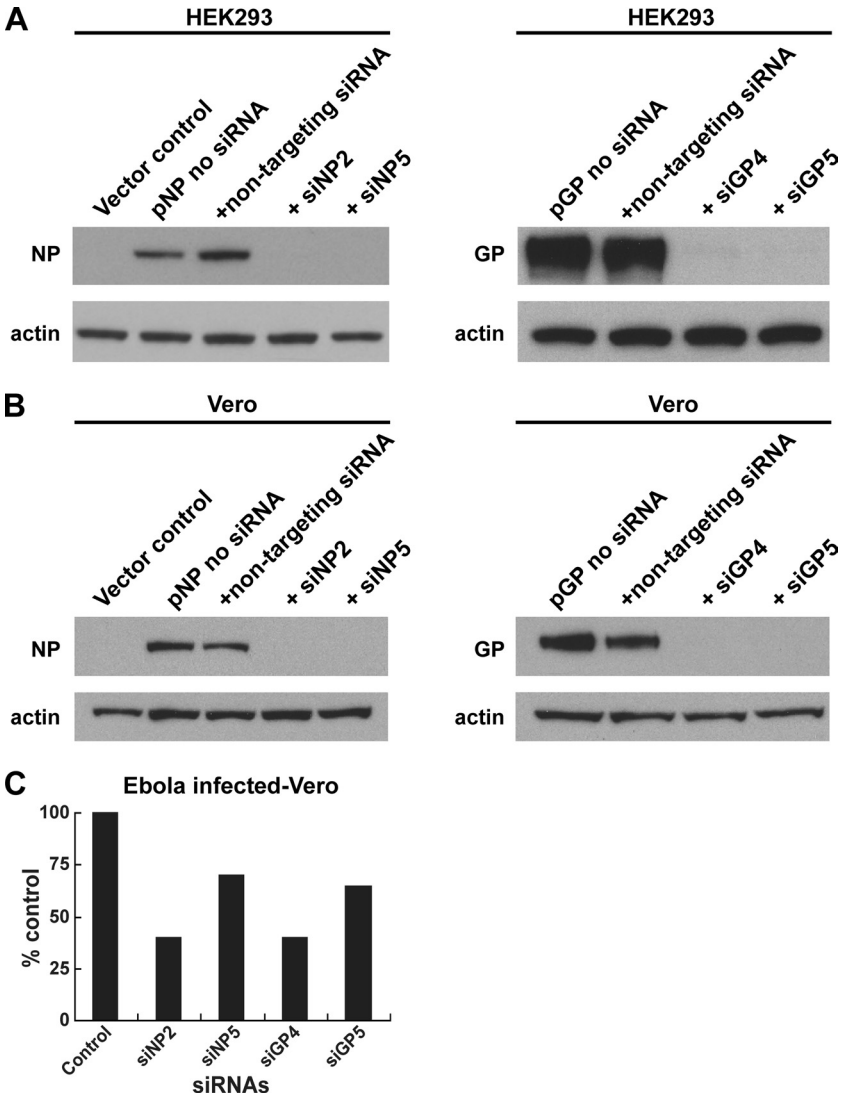

FIG. 1. siRNA-RNAi knockdown of EBOV genes. (A and B) HEK293 and Vero cells were transfected with plasmids encoding EBOV nucleoprotein (pNP) or glycoprotein (pGP) alone, together with the nontargeting siRNA, or with siRNAs targeting the viral mRNAs. Cell extracts were analyzed by SDS-PAGE, proteins were detected by Western blotting with antibody to either NP or GP, and expression levels were normalized against β-actin expression. The experiments were performed in triplicate. (C) Vero cells were transfected with siNPs or siGPs and, after 4 h, infected with EBOV at an MOI of 0.2. Results are presented as percentages of EBOV-infected cells in the presence of nontargeting siRNA. Values are averages ± standard deviations (SD) from at least two independent experiments.

EBOV SRSs, VP35, is an IFN antagonist, we asked whether the siRNAs used in the reporter RNAi assay were able to induce type I IFNs and, consequently, potentially affect the reversion of silencing. We measured the levels of IFN-α or -β in HEK293 cells under silencing conditions and compared these values to those in cells treated with poly(I · C) and poly(dA-dT). Despite the fact that IFNs are induced by transfected poly(I · C) and poly(dA-dT), we did not observe IFN-α/β induction by siRNA treatment (Fig. 2C). In conclusion, EBOV proteins reverted siRNA RNAi independently of IFN activation in nonimmune cells.

We next examined whether the EBOV proteins mediate RNAi suppression in a dose-dependent manner (Fig. 2D). We transfected 0.5, 1.0, and 2.0 μg of plasmid DNA encoding each viral protein (VP30, VP35, VP40, and NP) with constant amounts of the GFP reporter plasmid and siGFP. The NP protein control did not affect GFP silencing at any dose. As the ratio of plasmid DNA to siGFP increased, we observed increasing levels of GFP expression correlating with increasing levels of VP30, VP35, and VP40 gene expression, which indicates that EBOV protein-mediated suppression of GFP silencing was dose dependent (Fig. 2D).

To demonstrate reversion of silencing with a relevant viral gene, we modified the RNAi reporter assay by replacing GFP with EBOV GP, which was previously observed to be completely silenced when transiently expressed in HEK293 cells together with a GP-specific siRNA (Fig. 1). VP30, VP35, VP40, or NP was cotransfected with GP by the same methods used in the GFP assay, and three viral proteins were able to reverse GP silencing, whereas NP again had no effect (Fig. 2E).

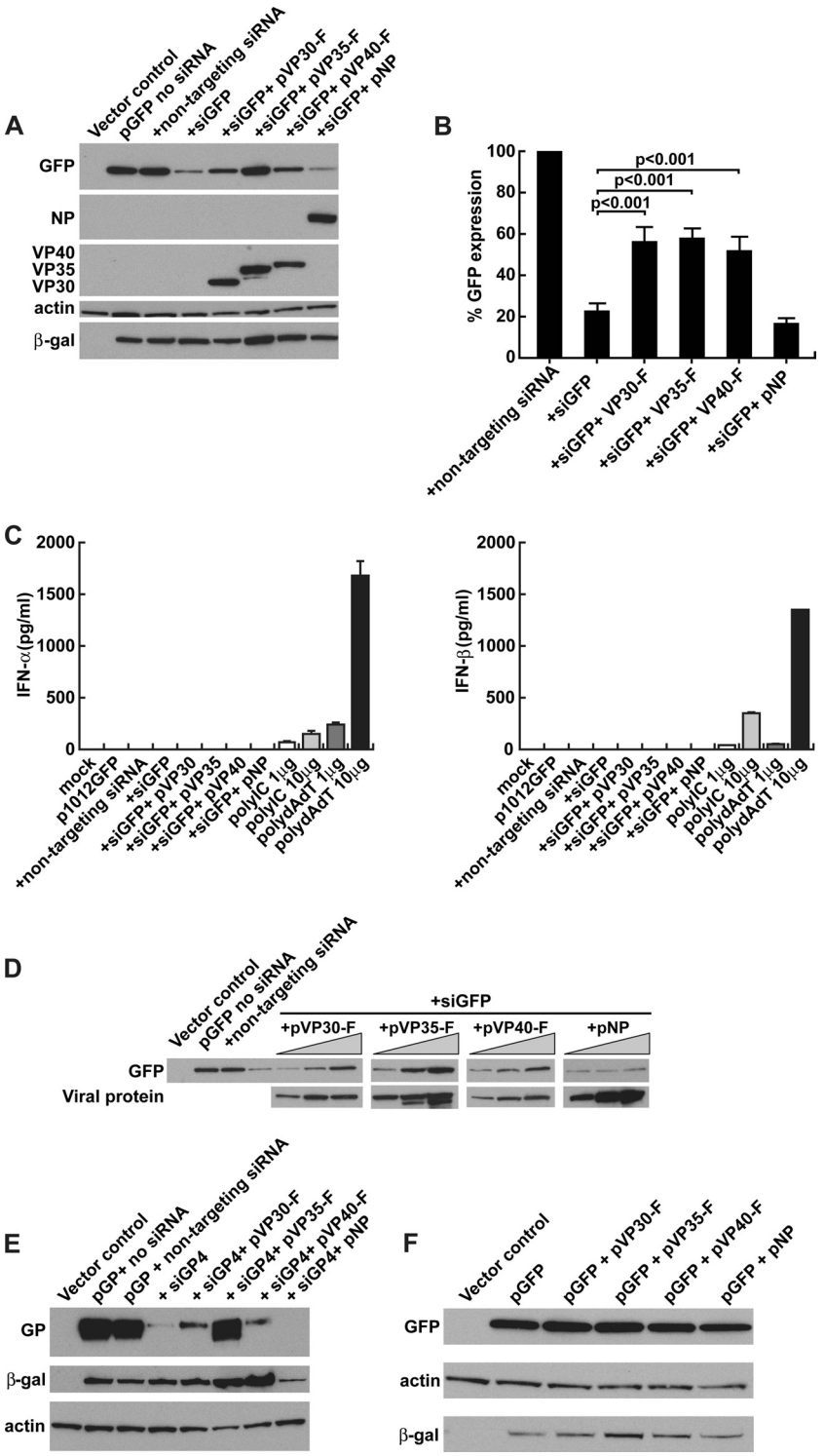

FIG. 2. Three EBOV products suppress siRNA-mediated RNA silencing. (A) Mammalian RNAi-based GFP reporter assay to screen EBOV proteins working as SRSs. pGFP was transfected into HEK293 cells alone, with the nontargeting siRNA, or with siGFP; plasmids encoding EBOV proteins were cotransfected with pGFP and siGFP. pVR1012 empty vector was transfected into HEK293 cells as a control. Plasmids pVP30, pVP35, and pVP40 with a C-terminal FLAG epitope are indicated by -F. pCMVLacZ and siGLO were cotransfected in each transfection mixture as controls for pDNA efficiency and for siRNA delivery and stability, respectively. Total cell lysates were subjected to SDS-PAGE followed by Western blotting with antibodies to GFP, NP, FLAG, β-actin, and β-Gal. A representative experiment of six is shown. Each sample was run in triplicate. (B) GFP expression quantified by densitometric analysis (ImageJ program) and normalized to β-Gal expression. Results represent the means ± SD from six independent experiments. Samples were analyzed with multiple-comparison repeated-measures one-way ANOVA with Student-Newman-Keuls *t* test (GraphPad Prism) to compute *P* values. Transfected β-Gal was used to normalize GFP expression; β-actin was used as a loading control. (C) siRNA treatment inhibits GFP expression without inducing a type I IFN (IFN-α/β) response. HEK293 cells were

Among the three viral proteins, VP35 and VP30 decreased siGP-mediated silencing at levels comparable to their effect on GFP reversion. The decrease in silencing by VP35 was 3.5-fold, whereas for VP30 and VP40 it was 2.5-fold. Taken together, these results confirmed that VP30, VP35, and VP40 all suppress siRNA-mediated RNAi independently of the target transcript.

We performed an additional experiment to confirm that suppression of RNAi was responsible for increased gene product expression, since several mechanisms could influence the translation of gene products. Trans-activating viral protein domains can mediate translational enhancement of host genes, and the multifunctional EBOV VP35 has been described to work as a translational enhancer (55). Therefore, we asked whether EBOV VP30, VP35, and VP40 act as translational enhancers of GFP expression and therefore account for the reversion of RNAi observed in our experimental conditions. To address this question, we coexpressed GFP in the absence of siGFP with these viral proteins together with a second reporter gene, such as β-Gal, used to control the efficiency of DNA transfection. If a protein works globally as a translational enhancer, it should enhance both reporter genes. EBOV NP protein was used as a control. We did not observe a significant increase in the level of GFP/β-Gal expression for EBOV SRSs VP30 and VP40 (Fig. 2F). However, cells expressing EBOV VP35 showed a marginal enhancement of GFP expression (20%) and some enhancement of the transfection control, pCMVLacZ, after normalization of GFP and β-Gal to actin (Fig. 2F). In light of this observation, we performed additional control experiments in the absence or presence of siGFP ($n = 12$) to understand whether or not the ability of VP35 to enhance gene reporter activity masked RNAi effects (data not shown). While there was a modest VP35-mediated enhancement of GFP (50%) in the absence of siGFP, this effect was not observed consistently, and the difference compared to the control result was not significant ($P > 0.05$). Moreover, the degree of enhancement was markedly lower than that observed for the VP35 effect on siRNA treatment (250%) ($P < 0.0001$). Overall, we concluded that while translational enhancement by VP35 could contribute to the increased expression of GFP, it does not account for the SRS function observed herein.

EBOV VP30 and VP35 have unique molecular interactions of RNAi suppression. To investigate how EBOV SRSs interact with RNAi, pilot experiments were performed to test interactions of viral proteins with siRNA using a streptavidin-biotin pulldown assay. The results indicated that VP30 and VP35 interact with siRNA-protein complexes but that VP40 did not (data not shown). Given the broad binding ability of the VP35 dsRBD, which has high affinity to either blunted or 5′ overhang dsRNAs (36), some degree of precipitation was observed using streptavidin in the presence of nonbiotinylated siRNA. Due to this limitation of the pulldown assay, we focused our investigation on the mechanism(s) employed by VP30 and VP35 for suppression of RNAi by direct immunoprecipitation of the viral proteins and components of RNAi.

We asked whether VP30 and VP35 interact with components of RNAi via protein-protein interaction or via an siRNA bridge. To distinguish between the two possible mechanisms, we coexpressed FLAG-tagged EBOV VP30 and VP35 in the presence or absence of pGFP and siGFP in HEK293 cells. Cellular extracts were subjected to immunoprecipitation with antibodies against Dicer, PACT, or TRBP and assayed for the presence of the viral FLAG-tagged proteins by Western blotting using an anti-FLAG antibody. The input amounts of each protein were comparable although slightly higher for VP35 than the other proteins (Fig. 3D). The results in Fig. 3A show that VP30 interacted with Dicer in either the presence or the absence of siRNA. However, less VP30 is coprecipitated with Dicer in the absence of siRNA than in the presence of siRNA. In contrast, VP30 interacted with TRBP only in the presence of siRNA (Fig. 3B). VP30 was not observed to associate with PACT, the other Dicer partner (Fig. 3C). Our immunoprecipitation method cannot resolve whether VP30 association with the RISC is via direct interaction with Dicer and TRBP or with siRNA, only that there is an association with the complex. Since VP30 associates with Dicer in the absence of siRNA, the association likely occurs through protein-protein interaction, and it suggests that the viral protein contacts (i) Dicer before it enters the siRNA pathway, (ii) Dicer-bound siRNA, or (iii) the pre-RISC loading complex. We observed that endogenous Dicer coprecipitated a lower level of VP30 in the absence of siRNA than with siRNA. This suggests that VP30 could form a complex that requires the participation of siRNA, such as the RISC. TRBP, Dicer, and Ago2 form the minimum human RISC loading complex *in vitro* (19). TRBP is required to recruit the Dicer-bound duplex siRNA to the Ago2-containing complex. The fact that the VP30 interaction seen with TRBP occurs in the presence of siRNA suggests that the viral protein is in a complex with Dicer and TRBP, which recruits Dicer-bound duplex siRNA to the Ago2-containing RISC. PACT, along with TRBP, Ago2, and Dicer, instead is in a 500-kDa

transfected with pGFP in the absence of siRNA, with nontargeting siRNA, with siGFP alone, or together with plasmids encoding viral proteins. Levels of IFN-α/β produced from HEK293 cells were measured by ELISA. Poly(I · C) and poly(dA-dT) were transfected with Lipofectamine into HEK293 cells and used as positive controls. One representative measurement of three is shown. (D) Reversion of GFP silencing is dose dependent. HEK293 cells were transiently transfected with pGFP alone or along with the nontargeting siRNA, with the siGFP, or with increasing amounts of each plasmid encoding the viral proteins (gray triangle). Total cell lysates were subjected to SDS-PAGE followed by Western blotting. EBOV VP30, VP35, and VP40 expression was detected with the anti-FLAG antibody, and NP expression was detected with a monoclonal antibody against NP. (E) EBOV RNAi suppressors block viral siRNA-mediated silencing. The plasmid pGP was transfected into HEK293 cells alone, with the nontargeting siRNA, with siGP4 targeting the GP mRNA alone, or with pVP30, pVP35, pVP40, or pNP. pVR1012 empty vector was transfected as a control. GP expression was measured by Western blotting using a GP antibody and normalized to β-Gal expression. β-Actin was used as a loading control. (F) EBOV proteins coexpressed with GFP in the absence of siRNA do not enhance reporter gene expression. pGFP and pLac, a second plasmid carrying a reporter gene used as a transfection control, were cotransfected into HEK293 cells alone or together with plasmids encoding EBOV proteins. pVR1012 empty vector was transfected into HEK293 cells as a control. Total cell lysates were subjected to SDS-PAGE followed by Western blotting with antibodies to GFP, β-actin, and β-Gal. GFP and β-Gal expression was normalized to endogenous β-actin expression (loading control). One experiment of two is shown (sample in triplicate).

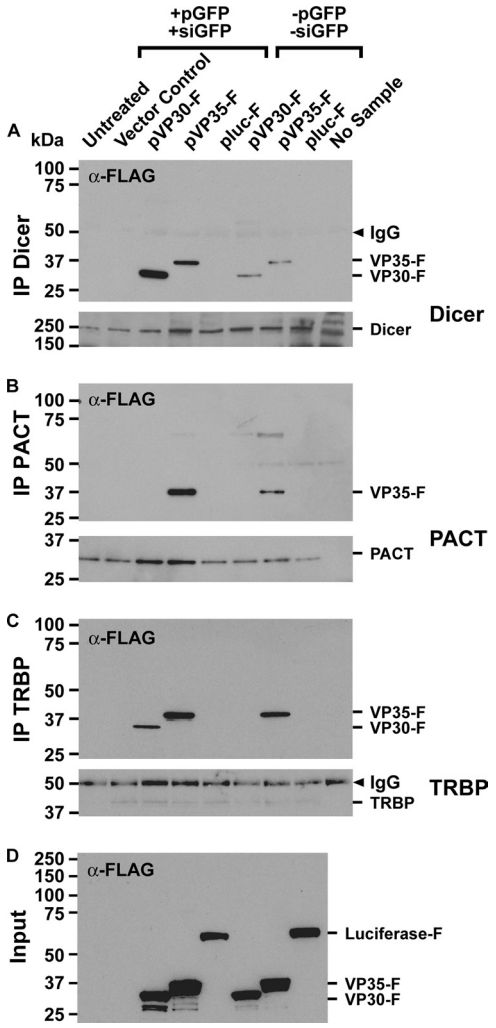

FIG. 3. Interactions of EBOV VP30 and VP35 with Dicer, TRBP, and PACT. FLAG-tagged VP30 and VP35 were coexpressed in HEK293 cells in the presence of pGFP together with siGFP or in the absence of pGFP and siGFP. An untransfected sample and empty vector (pVR1012) were used as negative controls. Immunoprecipitates were analyzed by SDS-PAGE followed by Western blotting using an anti-FLAG antibody (α-FLAG). Immunoprecipitation (IP) was carried out with anti-Dicer (A), anti-TRBP (B), and anti-PACT (C) antibodies. pluc-F was used as a negative control. Endogenous levels of Dicer, TRBP, and PACT were detected by probing with antibodies to Dicer, TRBP, and PACT. Input lanes contain 10% of the total cell lysates (D). This experiment was performed three times.

complex with target cleavage activity (33). The fact that VP30 does not associate with PACT suggests that VP30 may suppress RNAi before the active RISC.

The results in Fig. 3A to C show that VP35 associates with Dicer, TRBP, and PACT in the absence or presence of siRNA. However, as observed for VP30, less VP35 was coprecipitated with Dicer when siRNA was absent. These results indicate that VP35 contacts RNAi components through protein-protein interactions, suggesting that its SRS function does not absolutely require siRNA binding. Our immunoprecipitation data excluded the possibility that VP35 physically interfered with the TRBP-PACT complex, since if this were the case, the pulldown assay would have shown VP35 in a complex with only TRBP-Dicer or PACT-Dicer.

To determine whether VP35 interacts directly with Dicer, which in turn associates with the TRBP-PACT complex, or alternatively binds to TRBP and PACT, we transfected HEK293 cells with histidine (His)-tagged VP35 (pVP35-H) alone or together with each FLAG-tagged RNAi component (pDicer-F, pTRBP-F, and pPACT-F). Cellular extracts were immunoprecipitated with an antibody directed to the FLAG tag and analyzed by Western blotting with an antibody directed to the His epitope to detect the presence of viral protein VP35. As shown in Fig. 4A, TRBP and PACT coimmunoprecipitated with VP35. This result indicates that VP35 interacts with Dicer partners TRBP and PACT but not with Dicer.

To understand whether or not the dsRNA binding activity and IFN antagonist function mediated the suppressive role of VP35, we tested two mutants of VP35 (K309A and R312A mutants) previously shown to reduce dsRNA binding and shRNA-RNAi suppression (21). HEK293 cells were transfected with the pVP35(K309A)- or pVP35(R312A)-His mutant alone or together with each FLAG-tagged RNAi component (pDicer-F, pTRBP-F, and pPACT-F). Cellular extracts were immunoprecipitated with an antibody directed to the FLAG tag, followed by Western blot probing with an anti-His antibody to detect the presence of the mutant proteins (Fig. 4B). Like the wild-type protein, the K309A and R312A mutants interacted with the RNAi components TRBP and PACT, suggesting that these residues are not required to mediate such interactions with RNAi machinery (Fig. 4B) and that the dsRBD/IFN functions are not involved in the SRS function of VP35. However, they do not exclude the possibility that endogenous small RNAs, such as host cellular miRNAs, or the *cis*-natural antisense transcript (NAT) can mediate the interactions seen (11, 48). Overall, our data show that EBOV VP30 and VP35 have distinct molecular interactions with the RNAi pathway.

The RBD of VP30 is not required for RNAi suppression. EBOV VP30 has an N terminus disordered region containing a short region of basic residues (residues 26 to 32, RARSSSR) and a zinc finger motif preceded by arginine residues that has suggested a potential RNA binding activity. By generating N-terminal deletions of VP30 and point mutants, it has been shown that residues 27 to 40 are required for RNA binding (27). To understand whether the RNA-binding domain of VP30 plays a role in the ability of the viral protein to suppress RNAi, we have generated two mutants previously described (27). The first mutant has the region encompassing residues 1 to 40 deleted (VP30Δ1-40) and has no detectable RNA binding activity; the second mutant carries a point mutation (R40A) and has a 4-fold-reduced RNA binding activity.

We employed the RNAi reporter assay described above by transfecting His-tagged wild-type VP30 as well as the pVP30(Δ1-40)-H and pVP30(R40A)-H mutants. Both mutants decreased siGFP-mediated silencing when coexpressed individually with pGFP and siGFP at levels comparable with that of the wild type (3.0-fold). This result suggests that the RNA binding activity of VP30 does not participate in the RNAi suppression of VP30 (Fig. 5A).

Residues at the C terminus of VP30 do not mediate VP30 RNAi suppression. Our data revealed that VP30 is in a complex with Dicer and one Dicer partner, TRBP, suggesting that

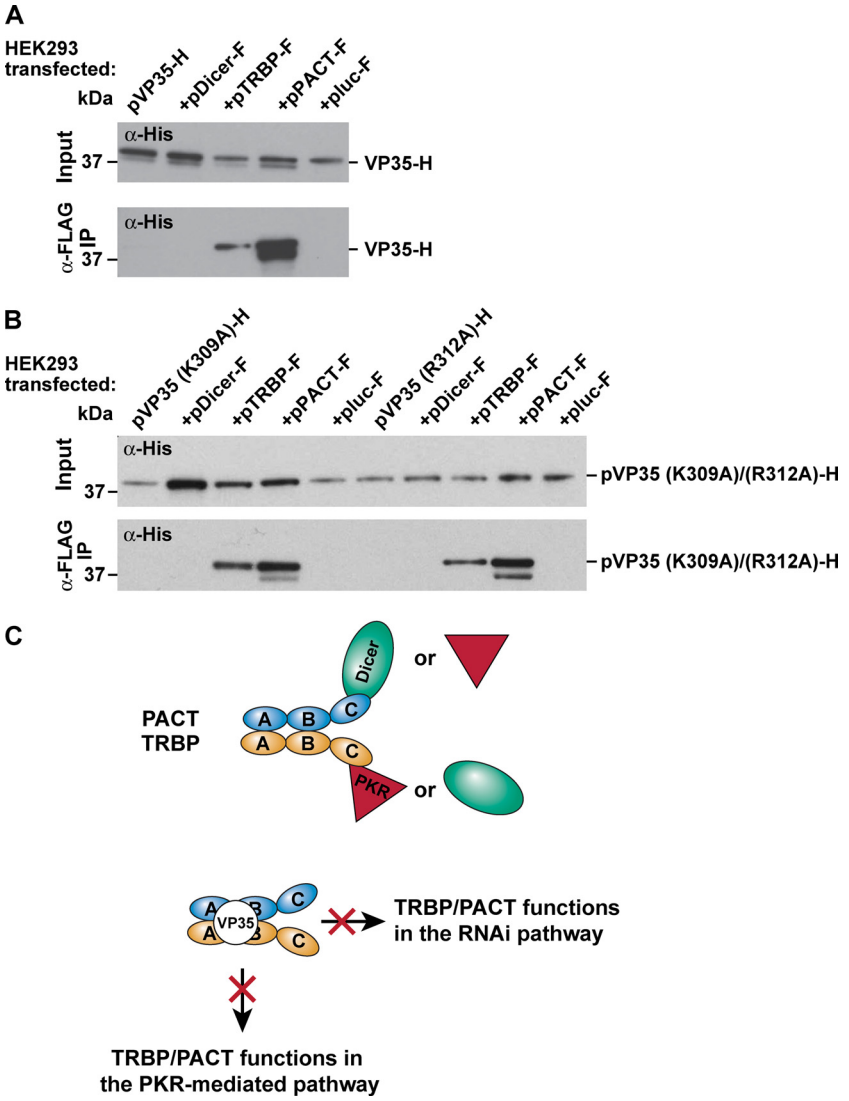

FIG. 4. EBOV VP35 interacts with TRBP and PACT: model for VP35. VP35 interacts with the Dicer/PKR partners TRBP and PACT but not with Dicer. (A) HEK293 cells were transfected with His-tagged pVP35 (pVP35-H) alone or with pDicer-F, pTRBP-F, or pPACT-F. Total cellular extracts were immunoprecipitated with anti-FLAG. Dicer, TRBP, and PACT immunoprecipitates were analyzed by SDS-PAGE followed by Western blotting using an anti-His antibody (α-FLAG IP). pluc-F was used as a negative control. Input lanes contain 10% of the total cell lysates and were detected with anti-His (Input). This experiment was performed three times. (B) Binding of dsRBD/IFN VP35 K309A and R312A mutants to TRBP/PACT. HEK293 cells were transfected with pVP35(K309A)- or pVP35(R312A)-His alone or with pDicer-F, pTRBP-F, or pPACT-F. Total cellular extracts were immunoprecipitated with anti-FLAG. Coimmunoprecipitation of VP35 mutants was detected using anti-His antibody (α-FLAG IP). pluc-F was used as a negative control. Input lanes contain 10% of the total cell lysates and were detected with anti-His (Input). (C) Molecular mechanism of VP35. By binding to Dicer/PKR partners, VP35 affects both RNAi and PKR pathways that require both TRBP and PACT. Domains of PACT and TRBP are shown as domains A, B, and C. TRBP-PACT heterodimer, domains A and B; Dicer (or PKR) binding, domain C. PACT, cyan oval; TRBP, yellow oval; Dicer, green oval; PKR, red triangle.

the protein interacts directly or indirectly with Dicer or TRBP, while TRBP passes the duplex siRNA to the RISC. VP30 could act at the level of RISC loading, at the step in which Dicer and TRBP contact the different ends of siRNA (44). The RNase IIIb domain of Dicer is able to interact with Ago2 (58) or with other RNAi components (Ago2-PACT). We hypothesize that an interaction with RNase IIIb might explain how VP30 limits the interaction between Dicer and PACT. This hypothesis was also suggested with a molecular model generated by performing a blind, rigid-body protein-protein docking between the crystal structure of the EBOV VP30 C-terminal domain dimer and the RNase IIIb domain dimer of human Dicer. Docking solutions favored placing VP30 within the RNA-binding groove of the RNase IIIb domains of Dicer. Among the cluster of solutions corresponding to the lowest energy configurations, three representative configurations were considered (data not shown). In one configuration, VP30 residues within contact distance of an Mg ion are D158, T161, E163, D164, and S165. In an alternative configuration, residues D202 and E205 of a VP30 C terminus monomer are present at a single Mg binding site. In a third configuration, amino acids H215 and S216 are near a single Mg binding site.

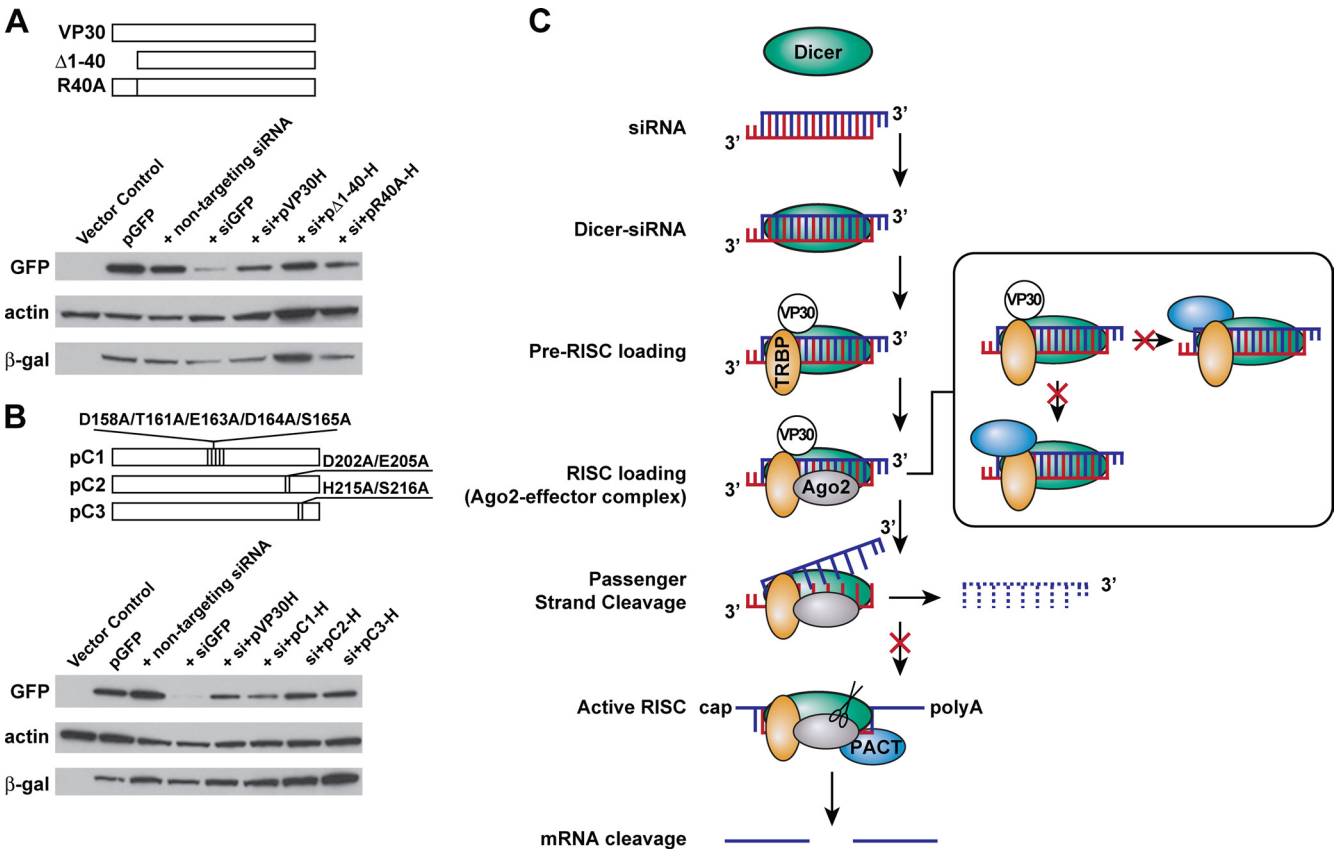

FIG. 5. EBOV RNAi suppression: model for VP30. (A) The RNA binding domain of VP30 does not mediate RNAi suppression. N-terminal mutants of VP30 (VP30Δ1-40 and the R40A mutant) were tested for their ability to abrogate the reversion of GFP silencing. pGFP was transfected into HEK293 cells alone, with the nontargeting siRNA, or with siGFP; plasmids encoding the wild-type protein VP30 (pVP30-H) or the N-terminal mutants were cotransfected with pGFP and siGFP. pVR1012 empty vector was transfected into HEK293 cells as a control. Plasmids pVP30, pVP30(Δ1-40) (pΔ1-40), and pVP30(R40A) (pR40A) with a C-terminal 6×His tag were used; pCMVLacZ and siGLO were cotransfected in each transfection mixture as controls for pDNA efficiency and for siRNA delivery and stability, respectively. Total cell lysates were subjected to SDS-PAGE followed by Western blotting with antibodies to GFP, β-actin, and β-Gal. A representative experiment of three is shown. Each sample was run in duplicate. (B) Point mutations at the C terminus of VP30 do not abrogate reversion of GFP silencing. Mutations were based on the molecular docking of the VP30 C terminus and the human Dicer RNase IIIb domain. Each alanine change is represented as a vertical line. pGFP was transfected into HEK293 cells alone, with the nontargeting siRNA, or with siGFP; plasmids encoding the wild-type protein VP30 (pVP30-H) or the C-terminal mutants were cotransfected with pGFP and siGFP. pVR1012 empty vector was transfected into HEK293 cells as a control. Plasmids pVP30, pC1, pC2, and pC3 with a C-terminal 6×His tag were used; pCMVLacZ and siGLO were cotransfected in each transfection mixture as controls for pDNA efficiency and for siRNA delivery and stability, respectively. Cell extracts were subjected to SDS-PAGE followed by Western blotting with antibodies to GFP, β-actin, and β-Gal. A representative experiment of three is shown. Each sample was run in duplicate. (C) Model for EBOV VP30 interaction with the RNAi pathway. The guide strand (red) and the passenger strand (blue) are shown. Dicer (green oval) senses the duplex siRNA by length and binds to it. TRBP (yellow oval) recruits the Dicer-bound siRNA to be loaded onto the Ago2-containing complex (gray oval). The RISC unwinds duplex siRNA and cleaves the passenger strand (blue dashed line). The guide strand (red) is loaded onto the active RISC, which contains PACT (blue oval). Ago2 cleaves the targeted mRNA (Ago2-slicing activity) (scissors). (Inset) Binding to Dicer or TRBP, VP30 limits contacts between Dicer and PACT or between TRBP and PACT.

Based on these data, we generated three VP30 mutant proteins (C1, C2, and C3) in which the residues interacting with the RNA-binding groove or present at the binding groove within coordinating distance of Mg ions were mutated to alanine. The VP30 mutant protein C1 carries D158A, T161A, E163A, D164A, and S165A mutations; the other two VP30 mutant proteins, C2 and C3, have D202A/E205A and H215A/S216A mutations, respectively. We employed the mammalian reporter RNAi assay to test the ability of these three VP30 mutant proteins to abrogate siRNA RNAi. All mutants decreased siGFP-mediated silencing when coexpressed individually with pGFP and siGFP at a level comparable with that of the wild-type protein (Fig. 5B). This result suggests either that these specific residues do not mediate the effect of VP30 to block RNAi or that RNAi suppression by VP30 does not require a direct interaction of the viral protein with Dicer. Further studies are required to identify which domain of Dicer in the complex TRBP–Dicer-bound siRNA is targeted by VP30, if the protein directly contacts Dicer. Additional mutagenesis of VP30 is required to assess how the viral protein contacts TRBP and prevents TRBP-PACT interactions.

DISCUSSION

Viruses have evolved several strategies to replicate successfully within an infected host while avoiding antiviral responses such as apoptosis, IFN, RNAi, and autophagy (2, 9, 23, 32).

Regardless of the host species or the genomic nucleic acid composition (RNA versus DNA), many viruses resist RNAi by encoding SRSs (37, 38, 56). In this study, we showed that EBOV encodes three proteins that suppress host RNAi-based immunity. We designed sequence-specific siRNAs that silenced viral genes expressed as RNA polymerase II-driven transcripts. When cells treated with the same siRNAs were infected with the virus, however, siRNA-mediated RNAi was unable to silence the same viral genes, suggesting that the virus possesses a mechanism to counter RNAi. Using a reporter-based RNAi assay, we identified VP30, VP35, and VP40 as SRSs.

We focused on identifying the molecular mechanisms by which VP30 and VP35 interact with the RNAi machinery and observed direct associations with components of RNAi. There are several features of the three proteins identified that support their role as SRSs in the context of the EBOV life cycle. (i) All SRSs identified to date are ssRNA- or dsRNA-binding proteins (36). All three EBOV protein candidates fit this paradigm. (ii) It is important to viral replication that any SRS should act early in the postentry life cycle to efficiently suppress the host RNAi apparatus. It is therefore of note that two of the three proteins identified, VP30 and VP35, are components of the EBOV RNP transcriptional replication complex. (iii) The exclusively cytosolic intracellular life cycle of EBOV leaves the viral genome accessible to the cytosolic RNAi machinery; the panhandle-like dsRNA may trigger host RNAi. Encoding multiple independent mechanisms to suppress RNAi might be necessary for a virus displaying such susceptibility.

Many known mammalian SRSs are dsRBPs and potent IFN antagonists. The SRS activity of EBOV VP35 has been postulated (21) based on the viral protein function as a dsRBP and IFN antagonist like other mammalian SRSs (38). By use of VP35 point mutants defective in dsRNA binding/IFN antagonism (R312A and K309A mutants) that abolish shRNA-RNAi suppression, it has been proposed that the dsRNA binding ability of VP35 mediates the SRS function (21). In this study, we observed that VP35 interacts with RNAi in an siRNA-independent fashion. We also found that transfected siRNAs do not induce IFNs in HEK293 cells (Fig. 2C). Thus, we propose that VP35 contains SRS functions independent of two other known properties of VP35, the dsRNA binding activity and IFN antagonism. Finally, our observations provide evidence that the dsRBP/IFN antagonist criterion (38, 61) is not universally applicable to all viruses.

Here, we report for the first time the molecular interactions between VP35 and RNAi machinery. Our data show that VP35 interacts with RNAi components through protein-protein interactions. VP35 is in a complex with Dicer and its partners TRBP and PACT and directly interacts only with Dicer partners. TRBP and PACT heterodimerize through domains A and B in an RNA-independent fashion and contact Dicer or PKR through domain C (Fig. 4C) (29, 33). VP35 simultaneously contacts TRBP-PACT, implying that this interaction occurs through domains A and B, which are not directly involved with Dicer or PKR binding. As a consequence, one of the Dicer partners (TRBP or PACT) can still interact with PKR, and this might explain previous results that failed to detect a physical interaction between VP35 and PKR (15), despite a reduction in PKR level, as well as residual IFN inhibition (5). Also, either TRBP or PACT can still bind to Dicer, present at any step of the RNAi pathway, e.g., at the dsRNA cleavage step. This might help to interpret results showing that VP35 suppresses shRNA-mediated RNAi (21). shRNAs, indeed, require Dicer cleavage or Dicer partners TRBP and PACT, which assist Dicer in this step (29). The use of VP35 mutants showed that point mutations K309A and R312A present at the C terminus of VP35 in the dsRNA binding/IFN domain are not required for the interaction with Dicer partners TRBP and PACT. Recently, structural data of the VP35 carboxyl-terminal IFN domain have suggested that additional basic residues may play a role in the dsRNA binding activity/IFN functions (34, 35).

Upon dsRNA-mediated IFN induction or viral infection, PKR is strongly enhanced, whereas PKR remains latent in unstimulated cells until activation is mediated by the cellular factor PACT (39). VP35 recruits TRBP and PACT, positive and negative regulators of PKR and partners of Dicer, which are shared between RNAi and the dsRNA/PKR recognition pathway. Though coimmunoprecipitation of VP35 with TRBP and PACT is an indirect demonstration of the suppressive role of VP35, we propose a model in which the viral protein mediates the cross talk between these two pathways by sequestering key components of host cellular RNA-mediated antiviral immunity (Fig. 4C). Despite the presence of viral dsRNA, VP35 employs a molecular mechanism that might result in more advantages in antagonizing host RNA defenses, not only affecting RNAi steps which require both TRBP and PACT (6, 19, 20, 33) but also regulating the PKR-mediated pathway. PKR, indeed, is activated by PACT (39). PACT-mediated PKR activation is regulated by TRBP concentration or by stress-induced dissociation of the TRBP-PACT complex (10).

The transcriptional factor VP30 also reveals a novel molecular mechanism of RNAi suppression. Though the association seen between VP30 and RNAi components cannot prove directly that the viral protein mediates the inhibition of RNAi, we have considered the interactions seen and the behavior of mutant proteins to propose a model. The important features of the model are the presence of an siRNA bridge in the interaction with TRBP and the absence of PACT association when VP30 is in a complex with RNAi components. Dicer interacts with VP30 regardless of the presence of siRNA. This interaction with Dicer and TRBP, but not PACT, suggests that VP30 prevents PACT from entering the RNAi machinery (Fig. 5C).

Our data favor a possible mode of action for VP30 in which the viral protein acts at the level of RISC loading and prevents any further RISC activity that requires PACT. By directly interacting with Dicer or with TRBP while TRBP passes the duplex siRNA to the RISC, VP30 limits the interactions between TRBP and PACT or between Dicer and PACT (Fig. 5C, inset). We hypothesize that VP30 may interfere with the TRBP–Dicer-bound siRNA complex at the level of RISC loading and that it intervenes at the step in which Dicer and TRBP contact the different ends of siRNA. By using mutants with mutations in the N terminus region of VP30, we have excluded the possibility that the RNA binding activity of the protein participates in RNAi suppression (Fig. 5A).

We tested the hypothesis that VP30 interacts with the RNase IIIb domain by using mutant proteins with mutations in the C-terminal region of VP30, carrying alanine changes in the

residues contacting the Dicer RNA-binding groove at or near the Mg ion-binding sites of Dicer. VP30 mutant proteins corresponding to the three predicted docking configurations of the VP30 RNase IIIb domain behave like the wild-type VP30 protein in reverting siRNA RNAi (Fig. 5B), suggesting either that these residues of VP30 do not mediate the effect of VP30 to block RNAi or that RNAi suppression by VP30 does not require a direct interaction of the viral protein with Dicer. Our result excludes the possibility that the interaction of VP30 with the Dicer RNase IIIb domain limits further interactions of Dicer with the Piwi domain of Ago2 (58) or with other RNAi components (Ago2-PACT). It might be possible that the viral protein interacts with other Dicer domains (e.g., PAZ). Alternatively, VP30 can directly interact with the TRBP-siRNA complex with which Dicer is in contact.

EBOV has developed redundant mechanisms to counterattack host RNAi-based immunity. We found a third SRS, the EBOV matrix protein VP40. Preliminary experiments show that VP40 was not seen in association with siRNA protein complexes, suggesting that it may function by a different mechanism. It has been shown that plant-infecting viruses encoding multiple SRSs may disable host RNAi in a temporal and cellular location-related manner during infection (43, 60). In mammalian cells, two Dicer-Ago2 complexes have been found to localize mainly in the cytosol and with a small but a significant fraction with the membrane (25, 58). We speculate a mode of action in which VP40 may recruit components of RNAi that are associated with the membranes but at levels too low for detection by immunoprecipitation. This is in accordance with the role played by VP40 during the late stages of the virus life cycle, when it interacts with the RNP complex and binds to the membrane during budding and virion release. Further studies will help to dissect the molecular mechanism by which VP40 blocks RNAi.

So far, mammalian RNAi suppressors have been studied by using overexpressed systems. Here, we demonstrate that overexpressed EBOV proteins suppress an experimentally initiated RNAi. One limitation of our study is that overexpressed proteins cannot address the physiological relevance of EBOV suppressors during infection. In addition, an overexpressed system limits the possibility to study in a temporal manner the role of a protein, such as the matrix protein VP40, known to be expressed later during infection, after the less abundant VP35 (13).

Here, we show that EBOV has evolved a mechanism to subvert RNAi, similar to what has been reported for influenza A virus and HIV-1 (3, 17, 40). It should be noted that EBOV replication and subsequent lethal effects in primates can be reduced by treatment with siRNA (18). However, siRNA treatment is required over time to maintain the efficacy, demonstrating a balance between viral replication and innate immune response by the host (18) and a potential role for EBOV SRSs.

EBOV is the first mammalian virus for which more than one SRS has been identified. So far, *Citrus tristeza virus* (CTV) is the only known plant-infecting virus to possess a sophisticated mechanism of RNA silencing suppression by encoding three SRSs (43). Regardless of genome polarity and the targeted host, EBOV- and CTV-encoded functions are either present early in the life cycle or abundantly expressed. SRSs from unrelated viruses have no sequence or structural similarity, even though they may have similar biochemical functions, suggesting that they have evolved independently (36). Consistent with this hypothesis, we observed that CTV p23 and EBOV VP30 possess an RNA binding activity within a region containing basic residues and a zinc finger domain (27, 42), suggesting that this is unlikely to be a mere coincidence; rather, it might be an example of an evolutionary convergence by which SRSs evolved independently such that they share a common function in distinct protein folds.

Why does EBOV have multiple SRSs? The simplest explanation may be grounded in the fact that EBOV contains multiple, distinct RNA-binding proteins that offer several opportunities to evolve antagonistic binding against host RNAi machinery. All three EBOV suppressors display potential unique binding specificities. We have confirmed this hypothesis by asking whether secondary structural elements related to the αββββα fold common to dsRBPs are present in EBOV SRSs. None of the three EBOV SRSs contain a dsRBD with the αββββα architecture. Thus, the absence of the canonical dsRBD fold suggests that RNAi suppressors undergo an independent evolution of protein folds to be able to bind RNAi activators.

Virus replication results in the release of many RNAs into the host cell cytosol. To prevent activation of RNA silencing, it may be more efficient for viruses to block RNAi protein effectors than to block the RNA stimuli, the latter of which could adversely affect virus propagation in the host. The identification of three viral SRSs demonstrates the importance of RNA-based immunity in the evolution of RNA viruses and provides important insight into viral pathogenesis and host defenses.

ACKNOWLEDGMENTS

We thank Ati Tislerics, Mythreyi Shastri, Rahul Roychoudhuri, and Abe Mittelman for editorial assistance, Michael Cichanowski for graphics, and all members of the Sullivan laboratory for helpful discussions. We thank the Bioinformatics and Computational Biosciences Branch (NIAID/NIH) for the fruitful collaboration, especially Kurt Wollenberg for the initial work on EBOV protein phylogenesis, Darrel Hurt for the three-dimensional models, and Vijayaraj Nagarajan for the secondary-structure predictions. We thank Tom Geisbert and Lisa Hensley for supporting the BSL4 experiment, Maria Tokuyama, Masaru Kanekiyo, Tracy Ruckwardt, and Brenna Hill for advice and critical discussions, Thomas Tuschl for the plasmid FLAG-Ago2, Narry K. Kim for the plasmids FLAG-Dicer, -PACT, and -TRBP, Bart Haynes for the monoclonal anti-NP-9B8, and Mary Kate Hart for the antibody anti-GP-12B5.

This work was supported by the Intramural Research Program, Vaccine Research Center, NIAID, NIH.

We have no financial conflicts of interest.

REFERENCES

1. **Ball, L. A.** 2001. Replication strategies of RNA viruses, p. 105–118. *In* D. M. Knipe, P. M. Howley, D. E. Griffin, M. A. Martin, R. A. Lamb, B. Roizman, and S. E. Straus (ed.), Fields virology, 4th ed. Lippincott, Williams & Wilkins, Philadelphia, PA.
2. **Benedict, C. A., P. S. Norris, and C. F. Ware.** 2002. To kill or be killed: viral evasion of apoptosis. Nat. Immunol. **3:**1013–1018.
3. **Bennasser, Y., S. Y. Le, M. Benkirane, and K. T. Jeang.** 2005. Evidence that HIV-1 encodes an siRNA and a suppressor of RNA silencing. Immunity **22:**607–619.
4. **Bitko, V., A. Musiyenko, O. Shulyayeva, and S. Barik.** 2005. Inhibition of respiratory viruses by nasally administered siRNA. Nat. Med. **11:**50–55.
5. **Cardenas, W. B., et al.** 2006. Ebola virus VP35 protein binds double-stranded RNA and inhibits alpha/beta interferon production induced by RIG-I signaling. J. Virol. **80:**5168–5178.
6. **Chendrimada, T. P., et al.** 2005. TRBP recruits the Dicer complex to Ago2 for microRNA processing and gene silencing. Nature **436:**740–744.
7. **Cole, C., J. D. Barber, and G. J. Barton.** 2008. The Jpred 3 secondary structure prediction server. Nucleic Acids Res. **36:**W197–W201.

8. **Combet, C., C. Blanchet, C. Geourjon, and G. Deleage.** 2000. NPS@: network protein sequence analysis. Trends Biochem. Sci. **25:**147–150.
9. **Cullen, B. R.** 2006. Is RNA interference involved in intrinsic antiviral immunity in mammals? Nat. Immunol. **7:**563–567.
10. **Daher, A., et al.** 2009. TRBP control of PACT-induced phosphorylation of protein kinase R is reversed by stress. Mol. Cell. Biol. **29:**254–265.
11. **Ding, S. W.** 2010. RNA-based antiviral immunity. Nat. Rev. Immunol. **10:**632–644.
12. **Elbashir, S. M., et al.** 2001. Duplexes of 21-nucleotide RNAs mediate RNA interference in cultured mammalian cells. Nature **411:**494–498.
13. **Elliott, L. H., M. P. Kiley, and J. B. McCormick.** 1985. Descriptive analysis of Ebola virus proteins. Virology **147:**169–176.
14. **Feldmann, H., and M. P. Kiley.** 1999. Classification, structure, and replication of filoviruses. Curr. Top. Microbiol. Immunol. **235:**1–21.
15. **Feng, Z., M. Cerveny, Z. Yan, and B. He.** 2007. The VP35 protein of Ebola virus inhibits the antiviral effect mediated by double-stranded RNA-dependent protein kinase PKR. J. Virol. **81:**182–192.
16. **Fire, A., et al.** 1998. Potent and specific genetic interference by double-stranded RNA in Caenorhabditis elegans. Nature **391:**806–811.
17. **Ge, Q., et al.** 2003. RNA interference of influenza virus production by directly targeting mRNA for degradation and indirectly inhibiting all viral RNA transcription. Proc. Natl. Acad. Sci. U. S. A. **100:**2718–2723.
18. **Geisbert, T. W., et al.** 2010. Postexposure protection of non-human primates against a lethal Ebola virus challenge with RNA interference: a proof-of-concept study. Lancet **375:**1896–1905.
19. **Gregory, R. I., T. P. Chendrimada, N. Cooch, and R. Shiekhattar.** 2005. Human RISC couples microRNA biogenesis and posttranscriptional gene silencing. Cell **123:**631–640.
20. **Haase, A. D., et al.** 2005. TRBP, a regulator of cellular PKR and HIV-1 virus expression, interacts with Dicer and functions in RNA silencing. EMBO Rep. **6:**961–967.
21. **Haasnoot, J., et al.** 2007. The Ebola virus VP35 protein is a suppressor of RNA silencing. PLoS Pathog. **3:**e86.
22. **Habjan, M., et al.** 2008. Processing of genome 5′ termini as a strategy of negative-strand RNA viruses to avoid RIG-I-dependent interferon induction. PLoS One **3:**e2032.
23. **Haller, O., G. Kochs, and F. Weber.** 2006. The interferon response circuit: induction and suppression by pathogenic viruses. Virology **344:**119–130.
24. **Hartikka, J., et al.** 1996. An improved plasmid DNA expression vector for direct injection into skeletal muscle. Hum. Gene Ther. **7:**1205–1217.
25. **Hock, J., et al.** 2007. Proteomic and functional analysis of Argonaute-containing mRNA-protein complexes in human cells. EMBO Rep. **8:**1052–1060.
26. **Hornung, V., et al.** 2006. 5′-Triphosphate RNA is the ligand for RIG-I. Science **314:**994–997.
27. **John, S. P., et al.** 2007. Ebola virus VP30 is an RNA binding protein. J. Virol. **81:**8967–8976.
28. **Kapadia, S. B., A. Brideau-Andersen, and F. V. Chisari.** 2003. Interference of hepatitis C virus RNA replication by short interfering RNAs. Proc. Natl. Acad. Sci. U. S. A. **100:**2014–2018.
29. **Kok, K. H., M. H. Ng, Y. P. Ching, and D. Y. Jin.** 2007. Human TRBP and PACT directly interact with each other and associate with dicer to facilitate the production of small interfering RNA. J. Biol. Chem. **282:**17649–17657.
30. **Kouranov, A., et al.** 2006. The RCSB PDB information portal for structural genomics. Nucleic Acids Res. **34:**D302–D305.
31. **Kumar, P., et al.** 2008. T cell-specific siRNA delivery suppresses HIV-1 infection in humanized mice. Cell **134:**577–586.
32. **Lee, H. K., and A. Iwasaki.** 2008. Autophagy and antiviral immunity. Curr. Opin. Immunol. **20:**23–29.
33. **Lee, Y., et al.** 2006. The role of PACT in the RNA silencing pathway. EMBO J. **25:**522–532.
34. **Leung, D. W., et al.** 2009. Structure of the Ebola VP35 interferon inhibitory domain. Proc. Natl. Acad. Sci. U. S. A. **106:**411–416.
35. **Leung, D. W., et al.** 2010. Structural basis for dsRNA recognition and interferon antagonism by Ebola VP35. Nat. Struct. Mol. Biol. **17:**165–172.
36. **Li, F., and S. W. Ding.** 2006. Virus counterdefense: diverse strategies for evading the RNA-silencing immunity. Annu. Rev. Microbiol. **60:**503–531.
37. **Li, H., W. X. Li, and S. W. Ding.** 2002. Induction and suppression of RNA silencing by an animal virus. Science **296:**1319–1321.
38. **Li, H. W., and S. W. Ding.** 2005. Antiviral silencing in animals. FEBS Lett. **579:**5965–5973.
39. **Li, S., et al.** 2006. Molecular basis for PKR activation by PACT or dsRNA. Proc. Natl. Acad. Sci. U. S. A. **103:**10005–10010.
40. **Li, W. X., et al.** 2004. Interferon antagonist proteins of influenza and vaccinia viruses are suppressors of RNA silencing. Proc. Natl. Acad. Sci. U. S. A. **101:**1350–1355.
41. **Liu, J., et al.** 2004. Argonaute2 is the catalytic engine of mammalian RNAi. Science **305:**1437–1441.
42. **Lopez, C., J. Navas-Castillo, S. Gowda, P. Moreno, and R. Flores.** 2000. The 23-kDa protein coded by the 3′-terminal gene of citrus tristeza virus is an RNA-binding protein. Virology **269:**462–470.
43. **Lu, R., et al.** 2004. Three distinct suppressors of RNA silencing encoded by a 20-kb viral RNA genome. Proc. Natl. Acad. Sci. U. S. A. **101:**15742–15747.
44. **Macrae, I. J., et al.** 2006. Structural basis for double-stranded RNA processing by Dicer. Science **311:**195–198.
45. **Meister, G., et al.** 2004. Human Argonaute2 mediates RNA cleavage targeted by miRNAs and siRNAs. Mol. Cell **15:**185–197.
46. **Meurs, E., et al.** 1990. Molecular cloning and characterization of the human double-stranded RNA-activated protein kinase induced by interferon. Cell **62:**379–390.
47. **Novina, C. D., and P. A. Sharp.** 2004. The RNAi revolution. Nature **430:**161–164.
48. **Parameswaran, P., et al.** 2010. Six RNA viruses and forty-one hosts: viral small RNAs and modulation of small RNA repertoires in vertebrate and invertebrate systems. PLoS Pathog. **6:**e1000764.
49. **Pollastri, G., and A. McLysaght.** 2005. Porter: a new, accurate server for protein secondary structure prediction. Bioinformatics **21:**1719–1720.
50. **Reynolds, A., et al.** 2006. Induction of the interferon response by siRNA is cell type- and duplex length-dependent. RNA **12:**988–993.
51. **Rost, B., G. Yachdav, and J. Liu.** 2004. The PredictProtein server. Nucleic Acids Res. **32:**W321–W326.
52. **Schlee, M., et al.** 2009. Recognition of 5′ triphosphate by RIG-I helicase requires short blunt double-stranded RNA as contained in panhandle of negative-strand virus. Immunity **31:**25–34.
53. **Schmidt, A., et al.** 2009. 5′-Triphosphate RNA requires base-paired structures to activate antiviral signaling via RIG-I. Proc. Natl. Acad. Sci. U. S. A. **106:**12067–12072.
54. **Schneidman-Duhovny, D.** 2005. PatchDock and SymmDock: servers for rigid and symmetric docking. Nucleic Acids Res. **33:**W363–W367.
55. **Schumann, M., T. Gantke, and E. Muhlberger.** 2009. Ebola virus VP35 antagonizes PKR activity through its C-terminal interferon inhibitory domain. J. Virol. **83:**8993–8997.
56. **Sullivan, C. S., and D. Ganem.** 2005. A virus-encoded inhibitor that blocks RNA interference in mammalian cells. J. Virol. **79:**7371–7379.
57. **Sullivan, N. J., A. Sanchez, P. E. Rollin, Z. Y. Yang, and G. J. Nabel.** 2000. Development of a preventive vaccine for Ebola virus infection in primates. Nature **408:**605–609.
58. **Tahbaz, N., et al.** 2004. Characterization of the interactions between mammalian PAZ PIWI domain proteins and Dicer. EMBO Rep. **5:**189–194.
59. **Tovchigrechko, A., and I. A. Vakser.** 2006. GRAMM-X public web server for protein-protein docking. Nucleic Acids Res. **34:**W310–W314.
60. **Vanitharani, R., P. Chellappan, J. S. Pita, and C. M. Fauquet.** 2004. Differential roles of AC2 and AC4 of cassava geminiviruses in mediating synergism and suppression of posttranscriptional gene silencing. J. Virol. **78:**9487–9498.
61. **van Rij, R. P., and R. Andino.** 2006. The silent treatment: RNAi as a defense against virus infection in mammals. Trends Biotechnol. **24:**186–193.
62. **Volchkov, V. E., et al.** 1999. Characterization of the L gene and 5′ trailer region of Ebola virus. J. Gen. Virol. **80:**355–362.
63. **Whelan, S. P., J. N. Barr, and G. W. Wertz.** 2004. Transcription and replication of nonsegmented negative-strand RNA viruses. Curr. Top. Microbiol. Immunol. **283:**61–119.
64. **Xu, N., B. Segerman, X. Zhou, and G. Akusjarvi.** 2007. Adenovirus virus-associated RNAII-derived small RNAs are efficiently incorporated into the RNA-induced silencing complex and associate with polyribosomes. J. Virol. **81:**10540–10549.
65. **Zamore, P. D.** 2004. Plant RNAi: how a viral silencing suppressor inactivates siRNA. Curr. Biol. **14:**R198–R200.